Available online at www.sciencedirect.com
SCIENCE DIRECT
Experimental Eye Research 79 (2004) 563–576
EXPERIMENTAL EYE RESEARCH
www.elsevier.com/locate/yexer

Distribution, spherical structure and predicted Mie scattering of multilamellar bodies in human age-related nuclear cataracts

Kurt O. Gilliland[a], Christopher D. Freel[a], Sonke Johnsen[b], W. Craig Fowler[c], M. Joseph Costello[a,*]

[a]*Department of Cell and Developmental Biology, University of North Carolina at Chapel Hill, Chapel Hill, NC, USA*
[b]*Department of Biology, Duke University, Durham, NC, USA*
[c]*Department of Ophthalmology, Duke University Eye Center, Durham, NC, USA*

Received 22 December 2003; accepted in revised form 7 May 2004
Available online 14 August 2004

Abstract

Purpose: To characterize multilamellar bodies (MLBs), determine their distribution along the optic axis and predict their potential Mie scattering within human age-related nuclear cataracts. Previous studies restricted to the equatorial plane have shown that MLBs are rare spherical objects that are 1–4 μm in diameter and covered by multiple layers of thin lipid-rich membranes.

Methods: Eight human aged transparent lenses were obtained from eye bank donors and eight human age-related nuclear cataracts were obtained immediately after extracapsular extraction. Each sample was Vibratome sectioned fresh into 200 μm thick sections that were fixed and embedded for light or electron microscopy. Light micrograph montages of the optic axis containing the juvenile, fetal and embryonic nuclei were examined. Mie scattering for random coated spherical particles was calculated based on assumed and measured particle parameters.

Results: Cells along the optic axis of the cataract contained approximately 7·5 times more MLBs as similar regions of the aged transparent lens, although these MLBs occurred with extremely low frequency. Cells of the aged transparent lens contained $1 \cdot 3$ MLBs mm^{-2}, while those of the cataract contained $9 \cdot 6$ MLBs mm^{-2}, which are equivalent to calculated densities of $5 \cdot 6 \times 10^2$ and $4 \cdot 1 \times 10^3$ mm^{-3}, respectively. While some MLBs were located within the cytoplasm near cell membranes, others were found away from membranes. The MLBs are distinct from circular profiles resulting from finger-like projections between adjacent cells. MLBs displayed varying geometries and cytoplasmic textures, although predominately spherical with interiors similar to adjacent fiber cell cytoplasm. These results are in agreement with previous theoretical analysis of light scattering from human lenses and with previous morphological studies examining the equatorial plane of the lens. Potential Mie scattering of spherical particles with the average properties of the observed MLBs and assumed refractive index properties was calculated to be forward scattering of as much as 20% of the incident light.

Conclusions: The observed low frequency and absence of clustering of MLBs in the equatorial plane and along the optic axis suggests that MLBs are most likely uniformly distributed throughout the embryonic, fetal and juvenile nuclei of age-related cataracts. Because of their size, distribution, textured cytoplasm and calculated Mie scattering, MLBs probably cause local fluctuations in refractive index in human lens nuclei and, therefore, are potential sources of low-angle, forward light scattering that could impair image formation.

Keywords: human nuclear cataract; light scattering; electron microscopy; histology; multilamellar bodies; transparent human lens; age-related cataract

1. Introduction

How the lens begins to lose its transparency and scatter light is not clearly understood. Many studies have concentrated on potential damage to the crystallins, the proteins that pack the cytoplasm of the differentiated organelle-free lens fiber cells. These proteins, which

* Corresponding author. Dr M. J. Costello, Department of Cell and Developmental Biology, University of North Carolina at Chapel Hill, Chapel Hill, NC, USA.
E-mail address: mjc@med.unc.edu (M.J. Costello).

0014-4835/$ - see front matter © 2004 Elsevier Ltd. All rights reserved.
DOI:10.1016/j.exer.2004.05.017

permanently remain in lens fiber cells once produced, can undergo irreversible damage if they are oxidized, glycosylated, carbamylated, deamidated, or cross-linked (Zigler, 1994; Hanson et al., 2000). If the proteins are cross-linked, they may form high molecular weight aggregates (Jedziniak et al., 1973, 1975, 1978). These protein modifications may lead to local changes in the index of refraction, which may in turn cause light to scatter (Benedek, 1971, 1997; Benedek et al., 1999). As fiber cells and their crystallins age without being replaced, their molecular pathology progresses, resulting in the development of the opacity of the cataractous lens. The patient often experiences an increase in glare and a loss of visual acuity. Scattering particles composed of damaged protein, however, have been difficult to visualize because of their small size and irregular shape. Electron microscopic studies have demonstrated that cytoplasm of both aged transparent lenses and nuclear cataractous lenses is smooth (Al-Ghoul and Costello, 1996; Taylor and Costello, 1999). This smoothness indicates that the proteins present, while potentially damaged and even fused into high molecular weight aggregates, are homogenous in distribution and not likely to be major light scattering particles (Taylor and Costello, 1999). Indeed some cataracts have been shown to contain rough, textured cytoplasm as seen by electron microscopy, but most cataracts appear smooth, even though they may scatter light by slit lamp examination (Al-Ghoul and Costello, 1996; Al-Ghoul et al., 1996; Taylor and Costello, 1999; Freel et al., 2002). Since cataract is a multifactorial disease, it is likely that there are other light scattering sources, such as larger particles, that might produce more significant amounts of scattered light.

Just as fiber cell cytoplasmic proteins are not replenished throughout life, fiber cell membranes synthesized early in life are not metabolized and can be subject to chronic oxidative damage (Spector, 1984; Spector, 1995; Truscott, 2000). Oxidation of these membranes may cause irreversible cellular pathology (Babizhayev et al., 1988). It is possible that membrane damage might result in scattering particles that are larger than the molecular scattering particles caused by protein damage. These larger particles may be more effective at producing large fluctuations in refractive index and scattering light than smaller particles.

The multilamellar bodies (MLBs) recently described are likely candidates for large scattering particles (Gilliland et al., 2001). They are rare spherical objects, occupy a volume fraction of only 3×10^{-5} of the cataract, range in size from 1 to 4 μm diameter with an average diameter of about 2·4 μm, and are found within the equatorial plane of the inner nuclei of the human lens. The name is derived from the multiple thin bilayer membranes that coat the surface. While these MLBs were reported at a low frequency and were difficult to visualize, they occurred in histological sections with about 7·5 times greater frequency in cataracts compared to aged transparent lenses (Gilliland et al., 2001). Because they are the only major structural features that have been observed within the nuclear core that are consistently different in cataractous and transparent human nuclei, the MLBs are considered to be potential sources for excess light scattering in age-related nuclear cataracts. Particles of this size and volume fraction were hypothesized to be present by van den Berg (1997) who also suggested that their major contribution would be low-angle scattering. Their lipid-rich outer layer and variably textured interior cytoplasm might be responsible for key fluctuations in the local index of refraction essential to produce significant light scattering (Gilliland et al., 2001; Tang et al., 2003). Although several theoretical treatments have been proposed to describe the scattering from particles of various sizes within the lens (Debye and Bueche, 1949; Benedek, 1971; Bettelheim, 1985), for widely separated large spherical particles the scattering theory developed by Mie about 100 years ago is appropriate (Mie, 1908). Mie provided an analytical solution of Maxwell's equations for scattering from coated spheres (Born and Wolf, 1959; Kerker, 1969). Results of Mie scattering calculations support the hypothesis of van den Berg (van den Berg, 1997; van den Berg and Spekreijse, 1999) that particles of similar size to the MLBs contribute to the low angle scattering.

The primary interest of the present study was to further characterize the MLBs within the core of nuclear cataracts and calculate the potential scattering. In the previous study MLBs in the embryonic and fetal nuclear regions were described as viewed in the equatorial plane of the lens. The distribution of MLBs was determined from histological sections as the number per unit area, and the Floderus equation was used to calculate the expected number of MLBs that might be present in a unit volume (Gilliland et al., 2001). In the current study, similar procedures were employed on a larger sample size than in the previous study, and, importantly, MLBs were quantified in the embryonic, fetal and juvenile nuclear regions in a plane containing the optic axis. MLBs along the optic axis are similar in geometry, size and distribution to those in the equatorial plane providing support for the hypothesis that these large particles are randomly distributed within the entire inner nuclear core of age-related nuclear cataracts. A portion of this work has been presented previously (Gilliland et al., 2002).

2. Materials and methods

2.1. Lenses

Eight non-diabetic, non-cataractous, aged, transparent donor human eyes (ages 34, 45, 50, 55, 59, 65, 66, 71; Fig. 1A) were obtained from the North Carolina Eye and Human Tissue Bank (Durham, NC) and transported within 12 h of death to the University of North Carolina at Chapel Hill, where the transparent lenses were dissected from the eyes and prepared for analysis. Eight cataractous human

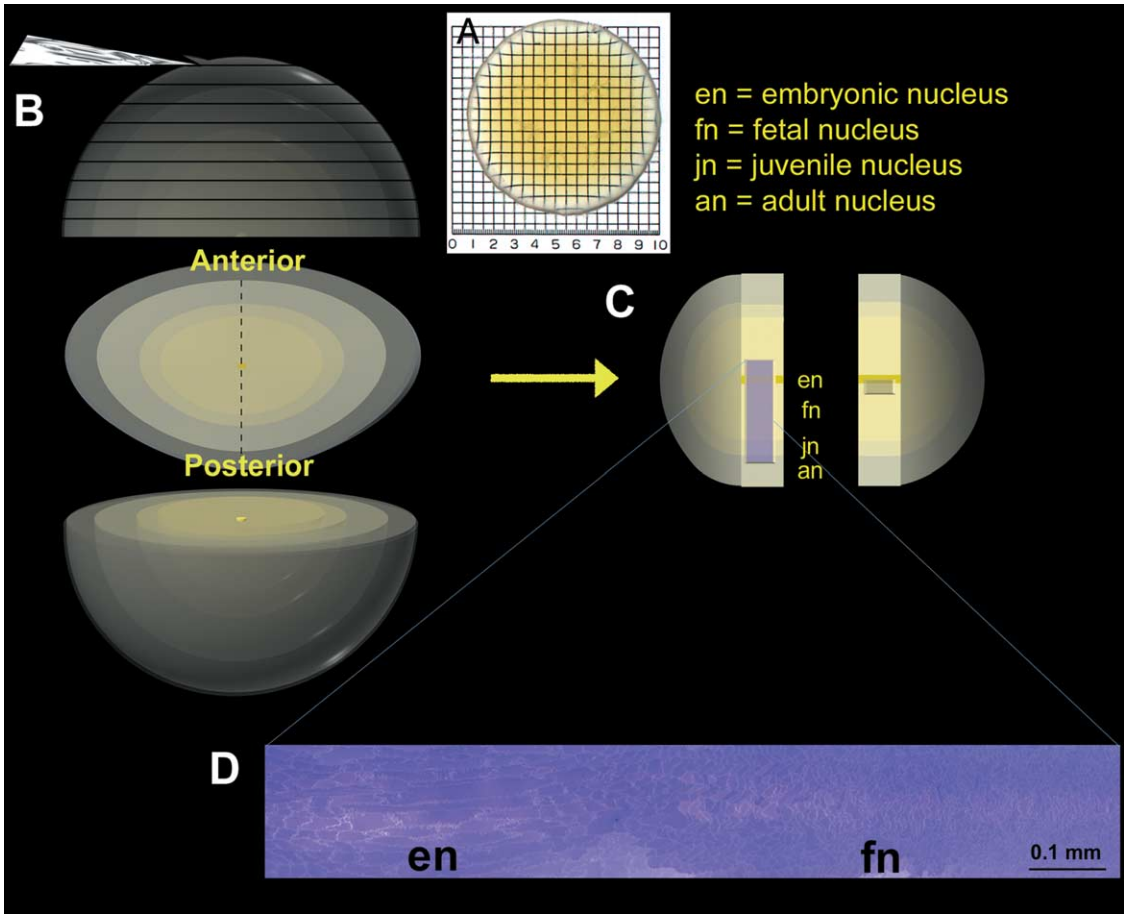

Fig. 1. Diagrams of the lens processing procedure. (A), Scan of a 55-year-old aged transparent donor lens. (B), Vibratome sectioning of an intact lens into 200 μm thick slices using a thin razor blade as the knife. The central section through the embryonic nucleus (en) is shown in face view where all developmental regions are visible (en, fn, fetal nucleus; jn, juvenile nucleus and an, adult nucleus) surrounded by the cortex. Sections of the nuclei from transparent lenses or from extracapsular extractions obtained in this study were bisected (dashed line) along the optic axis for further processing. (C), Vibratome section bisected along the optic axis. Long mesas (left) were used for preparing 0·7 μm thick sections for light microscopy. Small mesas (right) were used for preparing 70 nm thin sections for transmission electron microscopy. (D), Light micrograph montages, each $2{\cdot}6\times10^5$ μm^2 in area and 0·7 μm thick, were used to examine six sections in each of eight aged transparent human lenses and eight age-related cataractous nuclei.

nuclei (ages 56, 58, 72, 75, 81, 85, 85, 85) were obtained from the Duke University Eye Center (Durham, NC) after extracapsular cataract extraction. These cataracts were transported to the University of North Carolina at Chapel Hill the day of surgery and were prepared for analysis in the same fashion as the aged transparent lenses. The cataractous nuclei were not advanced, clinically graded by the surgeon from 1 to 3 (on a 0–4 scale for nuclear sclerosis), and the patients were not diabetic. Photographs of the type of nuclear cataract examined have been published previously (Al-Ghoul and Costello, 1996; Al-Ghoul et al., 1996). All specimens were collected following the tenets of the Declaration of Helsinki.

The anterior-to-posterior thickness and equatorial diameter of each lens nucleus were measured so that the center of the lens could be determined (Fig. 1A). Lenses were then mounted with cyanoacrylate glue onto a metal sectioning tray, covered with warm 2·5% agar, submerged in Tyrode's salt solution (Sigma, St. Louis, MO) at 10°C and sectioned using a vibrating knife microtome (TPI Vibratome model 1000, St. Louis, MO) at an amplitude of 7, a speed of approximately 0·2 mm/s and a cutting angle of 12° (Fig. 1B). Because of the precise sectioning process, the center section of each lens was collected for analysis.

2.2. Bright field and confocal fluorescent light microscopy

Vibratome sections approximately 200 μm thick were fixed for 12–18 h in 0·5% glutaraldehyde, 2% paraformaldehyde and 1% tannic acid in 0·1 M cacodylate buffer (pH 7·2). Sections were then washed with deionized distilled water for three 15-min washings, stained in 2% aqueous uranyl acetate in the dark for 60 min, washed with deionized distilled water once for 10 min and dehydrated through a graded ethanol series. Sections were infiltrated and embedded in LR White resin (Electron Microscopy Sciences, Ft. Washington, PA), from which histological sections (0·7 μm thick) of the nuclei were cut along the optic axis (Fig. 1C) and mounted on glass slides. Mounted sections were stained with toluidine blue oxide (TBO),

cover slipped and examined with a Leica DMR brightfield microscope (Solms, Germany). Digital images were collected with a Leica DC500 camera (Solms, Germany) (Fig. 1D).

Sections of 5–7 μm were cut from fixed and LR White embedded Vibratome sections on a microtome using a glass knife and placed onto glass slides. The sections were heated and stained with the lipophilic dye, DiI (1,1-dioctadecyl-3,3,3',3'-tetramethylindocarbocyanine perchlorate; Molecular Probes, Inc., Eugene, OR) following the procedures published previously (Boyle and Takemoto, 1997). Optical sectioning on a Zeiss LSM-410 (Carl Zeiss, Inc., Thornwood, NY) laser scanning confocal microscope was used to examine the tissues.

2.3. Transmission electron microscopy

Vibratome sections approximately 200 μm thick were fixed for 12–18 h in 2·5% glutaraldehyde, 2% paraformaldehyde and 1% tannic acid in 0·1 M cacodylate buffer (pH 7·2). Sections were then washed with 0·1 M cacodylate for three 15-min washings, treated with cold 0·5% osmium tetroxide for 60 min, washed with deionized distilled water for three 15-min washings, washed once with 50% ethanol for 5 min, stained in 2% uranyl acetate (ethanol-based) in the dark for 30 min and dehydrated through a graded ethanol series. Sections were infiltrated and embedded in an epoxy resin. Thin sections (70 nm) were cut with a diamond knife (Diatome US, Fort Washington, PA) from mesas raised to include the embryonic nucleus along the optic axis (Fig. 1C). Thin sections were stained with uranyl acetate and lead citrate for viewing at 80 kV on a FEI-Philips Tecnai 12 (FEI Company, Hillsboro, OR) transmission electron microscope.

2.4. Quantitative analysis

For each lens, six histological sections were examined. Within each of these 0·7 μm thick sections, a rectangular region (approximately 160 μm in width and 1580 μm in length) containing the embryonic, fetal and juvenile nuclear regions was thoroughly searched. Thus a total area of approximately 1·5 mm^2 was examined for each lens. MLBs were counted, ensuring that the same MLB was not counted twice in serial sections. The data were analysed statistically using StatView version 5·0 (SAS Institute, Inc., Cary, NC), employing the non-parametric Mann–Whitney test, appropriate for data with small n, which shows trends that were considered significant for $p<0·05$.

The Floderus equation was used to determine the numerical density (N_V) of the MLBs (Bozzola and Russell, 1999; Gilliland et al., 2001). The number of MLBs per unit area (N_A, measured data), section thickness ($T=0·7$ μm), average diameter of an MLB ($d=2·13$ μm, measured average) and height of the cap ($h=1/3$ the section thickness, or 0·23 μm) allow the numerical density to be calculated

$$N_V = N_A/(T + d - 2h) \quad (1)$$

The height of the cap is the smallest observed profile in the section and serves as a correction factor for the small polar regions of a sphere that become lost to the eye, because they are grazed during sectioning and therefore are present only in part of one section (Bozzola and Russell, 1999).

2.5. Calculation of Mie light scattering

The amount of light scattered by a single MLB is equal to QA, where Q is the scattering efficiency of the MLB and A is its cross-sectional area. Because the volume fraction of the MLBs in the lens is quite small (3×10^{-5}), they can be considered as independent scatterers. Therefore the total light scattered by N MLBs equals NQA. In the central square millimeter of the embryonic nucleus, N is equal to ρt, where ρ is the density of MLBs (mm^{-3}) and t is the thickness of the nucleus. Since the MLBs are spherical, A is equal to πr^2, where r is the radius of an MLB. Therefore, the total amount of light scattered by the MLBs in the center of the embryonic nucleus is

$$S = \rho t Q \pi r^2 \quad (2)$$

Since the central square millimeter has unit area, Eq. (2) also gives the fractional amount of light scattered.

The scattering efficiency of spherical MLB particles can be accurately calculated using the Mie scattering theory for coated spheres (Kerker, 1969). This theoretical description of scattering from spheres is based on an exact solution of Maxwell's equations for electromagnetic theory and is a detailed analysis of the diffraction of waves of light by a sphere of any size and composition as long as it is a homogeneous sphere in homogeneous surroundings.

The calculations are based on particular assumptions. For instance, the spheres should be separated from each other by distances that are large in comparison to the wavelength of incident light, and they should be of the same diameter and composition. While MLBs appear to be random in distribution and separated by great distances, they show some variation in size and composition. For this analysis, an average MLB diameter and refractive index have been assumed. In the specific case of age-related nuclear cataracts, the scattering efficiency depends on the wavelength of the incident light, the refractive index of the medium, and the refractive index and thickness of both the MLB and the lipid layer which forms the 'coat' of the MLB. In this case, the analytical solution was performed with the computer language C in Matlab 6·2 (Mathworks. Inc.), using algorithms developed by Mätzler (2002). In addition to calculating the scattering efficiencies, the algorithms also calculated the intensity and angular distribution of the scattered light.

3. Results

To obtain information about the distribution of MLBs within the volume of the lens nucleus, a study by light microscopy was designed to characterize the distribution of these spherical structures in planes parallel to and containing the optic axis. About $1 \cdot 5\ mm^2$ was examined carefully for each of eight aged transparent human lenses and for an equivalent area in each of eight human age-related nuclear cataracts. The results demonstrate that cells along the optic axis contain few MLBs and they appeared to be randomly distributed, indicated by the lack of order or clustering and by the large separation between individual MLBs. These features of the distribution were similar to the MLBs in fiber cells of the equatorial plane (Gilliland et al., 2001). A representative montage of a histological section of the aged transparent human lens along the optic axis reveals the longitudinally sectioned cylindrical primary fiber cells of the embryonic nucleus flanked by the secondary fiber cells of the fetal nucleus which are seen in cross section (Fig. 2A and C). A comparable montage of human age-related nuclear cataract, also viewed near the optic axis, displays cells that are similar in morphology to those of the aged transparent lens (Fig. 2B and D). No MLBs were found in the montages of the transparent lens (Fig. 2A and C). Note that the numerous small particle-like objects in some embryonic nuclear cells are probably due to interdigitations exposed by a tangential section at the cellular interface.

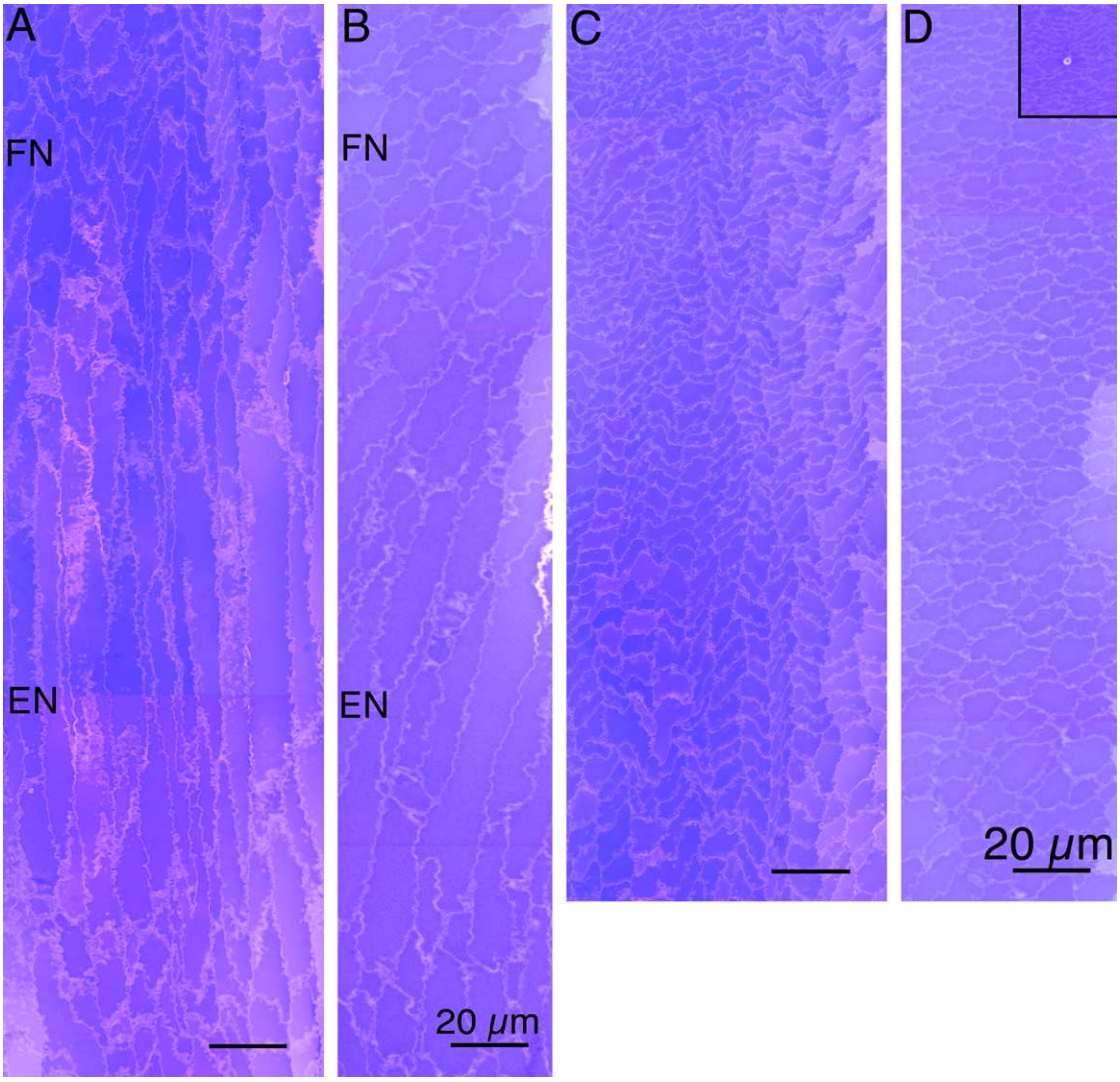

Fig. 2. Histological montages. (A,C), Aged transparent human lens and (B,D), human age-related nuclear cataract. The aged transparent human lens (A,C) is seen as viewed along the optic axis. The primary fiber cells of the embryonic nucleus (EN) are the long cylindrical cells located in the middle of the montage, surrounded by secondary fiber cells of the fetal nucleus (FN), which are seen in cross section above the embryonic nucleus. The human age-related nuclear cataract (B,D), also viewed along the optic axis, displays cells that are similar in morphology to those of the aged transparent lens, although a seldom-occurring multilamellar body (MLB) is located farther along the montage (D, inset, at the same magnification). The top of montages A and B continue at the bottom of montages C and D, respectively.

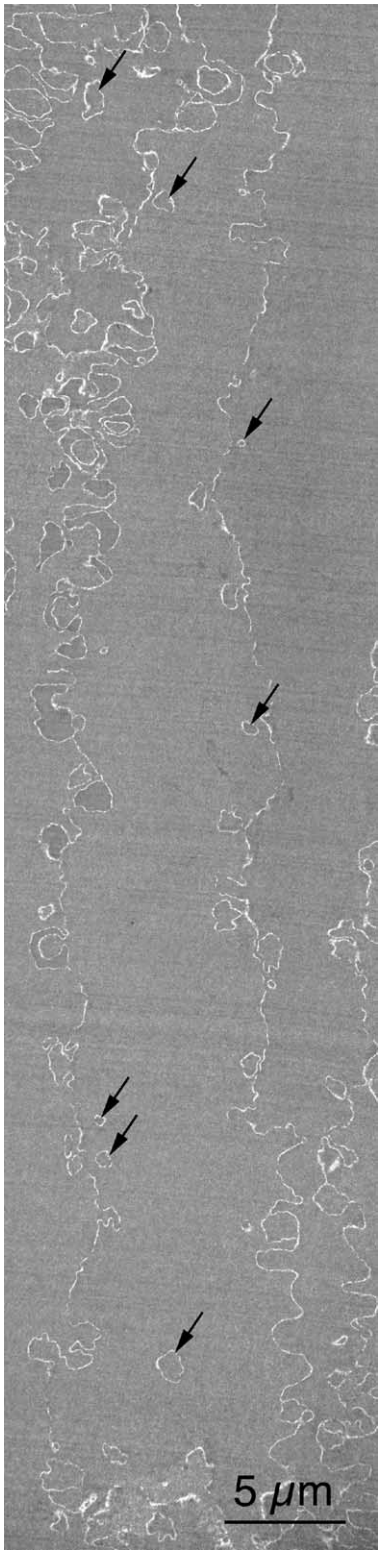

Fig. 3. Electron micrograph of a cataractous nucleus. A fiber cell from the embryonic nucleus of an age-related cataract is seen along its axis parallel to the optic axis. The undulations of the membrane are evident, as are the circular profiles (arrows), which represent the tip of finger-like projections of one cell into an adjacent cell. This particular cell contains no MLB. Such low magnification TEM images of the inner nucleus confirm that cell shape contours are similar in the aged transparent lens and the age-related cataract.

For the montage of the cataract, only one MLB was observed (Fig. 2D, inset), although it was located an additional 400 μm farther from the edge of the montage.

When viewed along the optic axis by transmission electron microscopy, fiber cells from the embryonic nucleus of the cataract (Fig. 3) appear similar to those of the aged transparent lens (data not shown). The longitudinal sections of fiber cells in the embryonic nucleus confirm that the plane of section passes along (or very close to) the optic axis. Also evident in the transmission electron micrographs of the longitudinal sections is the cell size, shape and interdigitation pattern, which is consistent with images obtained with light microscopy (Fig. 2) and scanning electron microscopy (Al-Ghoul et al., 2001). The images also demonstrate that both the cataract and the aged transparent lens contain membrane undulations and numerous circular profiles (Fig. 3, arrows) representing the tip ends of finger-like projections of one cell into an adjacent cell. These circular profiles, which are bounded by paired plasma membranes, are distinct from MLBs (Gilliland et al., 2001). An MLB from within the fetal nucleus of a cataractous lens is seen by transmission electron microscopy in Fig. 4. A high magnification view (Fig. 4, inset) demonstrates that the multiple layers of thin, tightly packed lipid membranes are each about 5 nm thick. Three layers are visible here and up to 10 layers have been seen in other MLBs. Most MLBs observed in the embryonic, fetal and juvenile nuclei along the optic axis appear similar to those in the equatorial plane (Gilliland et al., 2001). Whereas some are spherical in shape (Fig. 5A, B, D, H and I), others are composed of two or more conjoined spherical units (Fig. 5C, E–G and J). Evidence to support the hypothesized spherical geometry of a majority of the unique core structures is provided by the examination of one doublet structure (Fig. 6A–C) traced through *Z*-axis optical sections in about 0·5 μm steps by confocal microscopy (Fig. 6D). In the first step, the MLB is barely present, while in the second, third, fourth and fifth steps, it appears to be growing larger, achieving its maximum diameter in the fifth step. In the sixth, seventh and eighth steps, it becomes smaller until finally in the ninth step, it is hardly observable. Therefore, it appears that each component of the doublet is nearly spherical.

The analysis of histological sections indicates that MLBs occur with approximately 7·5 times greater frequency along the optic axis in the cataractous nuclei compared to the nuclei of the transparent lenses (Table 1). In each of eight transparent and eight cataractous nuclei, about 1·5 mm^2 of juvenile, fetal and embryonic nuclear regions was searched in the light microscope using high magnification objectives. A majority of aged transparent lenses yielded only 1 or even 0 MLBs per sample in the entire area searched, but one aged transparent lens contained as many as 5 MLBs. Such transparent lenses may contain MLBs that have not been altered with aging sufficiently to developed into major scattering centers. While some cataracts contained fewer than 8 MLBs in

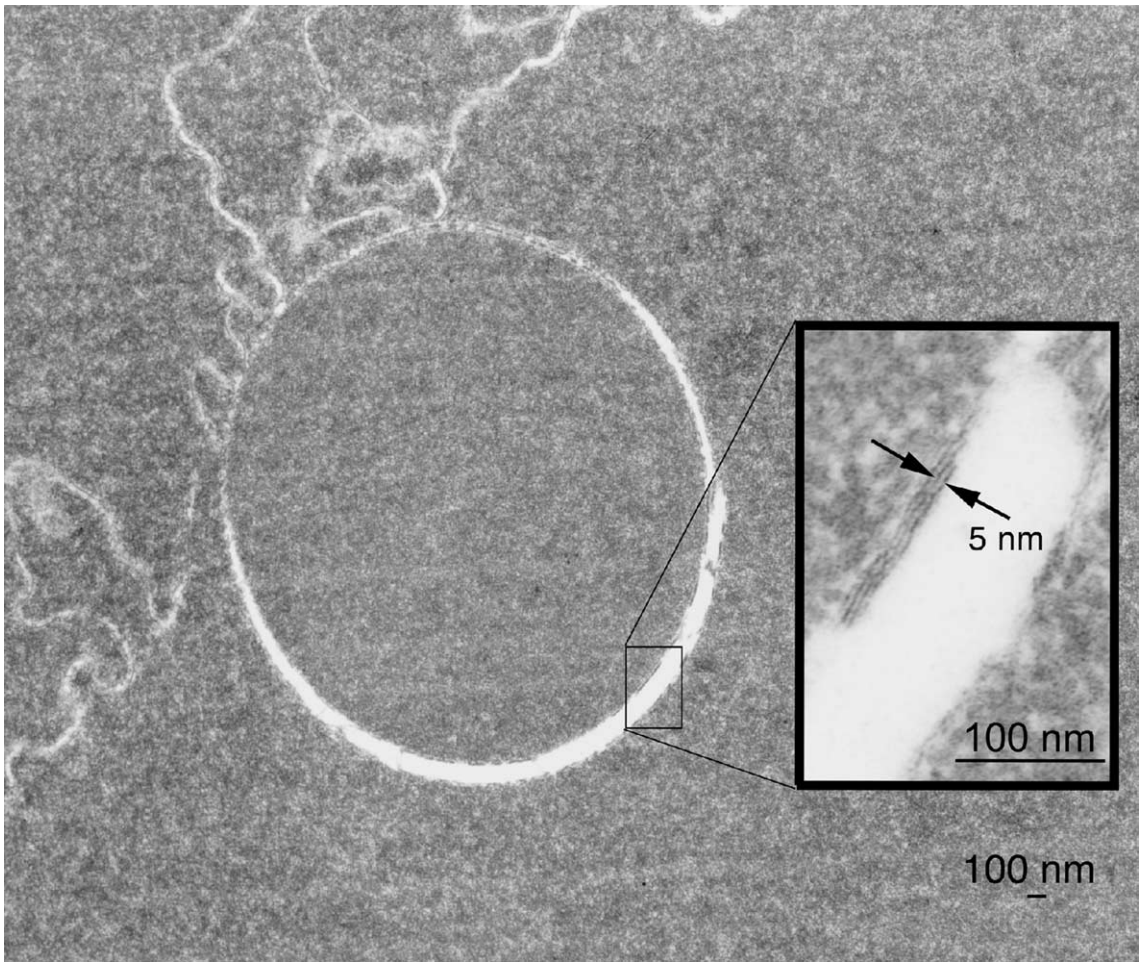

Fig. 4. Electron micrograph of an MLB. An MLB that is adjacent to plasma membranes from within the fetal nucleus of a cataractous nucleus is seen in a 70 nm thin section. The inset, a high magnification view of the boxed region, reveals that the MLB is surrounded by multiple layers of thin, tightly packed lipid membranes. The space between the arrows is 5 nm.

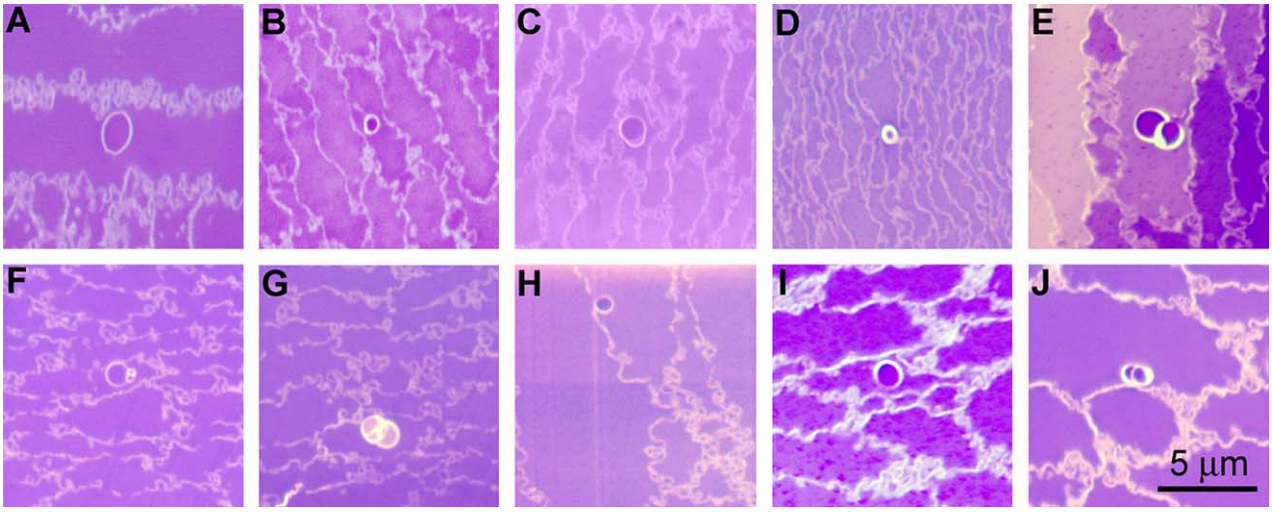

Fig. 5. A gallery of MLBs in light micrographs. MLBs are nearly spherical in shape (A, B, D, H and I), although some display unusual doublet or triplet geometries (C, E, F, G and J). The MLBs in A and H are from the embryonic nucleus and the others are from the fetal nucleus. MLBs are found with 7·5 times greater a frequency in the cataracts (B through J), although they do occur occasionally in aged transparent lenses (A). Note that the MLB in D is a magnified view of the MLB in the montage of the cataract (Fig. 2D).

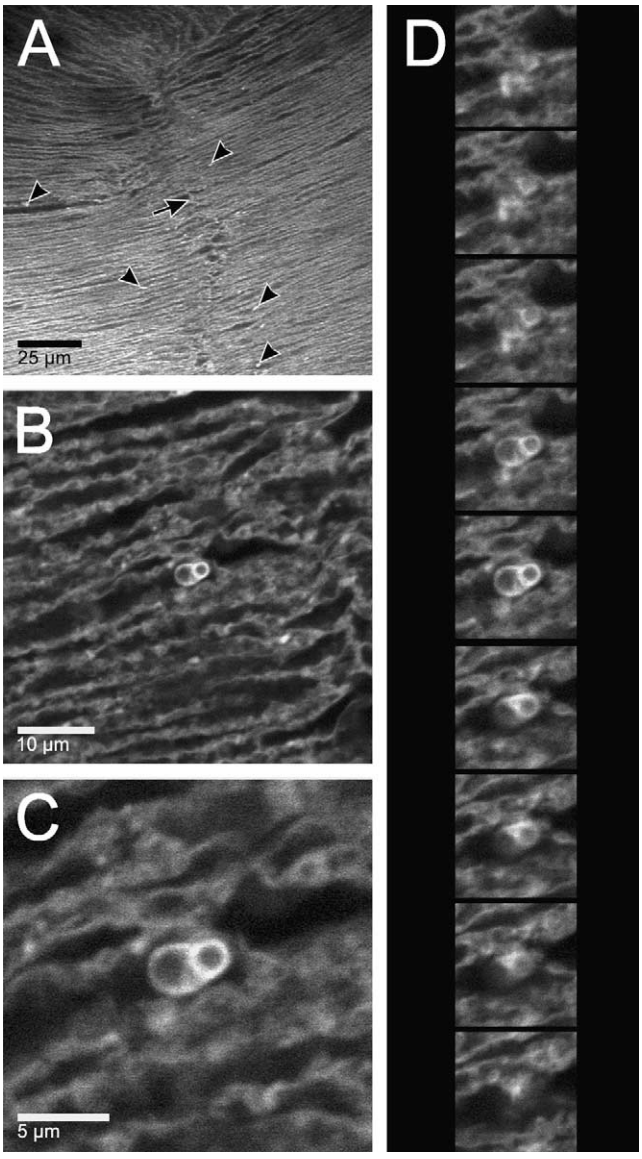

Fig. 6. Confocal images of a Vibratome section from a human nuclear cataract. (A), Overview of a suture (arrow) within the fetal nucleus. Bright spots (arrowheads) indicate high intensity fluorescence from the lipophilic dye DiI. (B), One of the bright spots at high magnification demonstrating the geometry and staining characteristic of MLBs. (C), Higher magnification of the MLB at the optimum optical slice to show the overall size of each spherical domain (3·0 µm diameter for left domain, 2·1 µm for right). (D), Z-axis optical sections in about 0·5 µm steps supporting the visual impression that the MLB contains spherical domains.

the area examined, most cataracts contained more than 8 and one cataract contained 60 MLBs. For a total of over 12 mm^2 of histological sections examined in the 8 cataracts, a total of 117 MLBs were observed, whereas only 16 MLBs were seen in similar regions of aged transparent human lenses (Table 1). Normalizing to the MLBs per unit area examined, the cataracts contained 9·6 MLBs mm^{-2}, whereas the aged transparent lenses yielded only 1·3 MLBs mm^{-2} (Table 1). The Mann–Whitney statistical test for small n supports the trend that

Table 1
Comparison of MLB frequency along the optic axis

Age (years)	MLBs	MLBs mm^{-2}
Aged transparent lenses		
34	3	2·0
45	5	3·3
50	1	0·7
55	1	0·7
59	4	2·6
65	1	0·7
66	0	0·0
71	1	0·7
Total	**16**	
Average		**1·3**
Cataractous lenses		
56	7	4·6
58	5	3·3
72	60	39·5
75	8	5·3
81	11	7·2
85(a)	14	9·2
85(b)	5	3·3
85(c)	7	4·6
Total	**117**	
Average		**9·6**

Greater than 1·52 mm^2 of juvenile, fetal and embryonic nuclear regions were searched in each of eight aged transparent lenses and eight cataractous nuclei. Comparing the MLBs per area examined, the cataracts exhibited 9·6 MLBs mm^{-2} (calculated density of $4{\cdot}1\times10^3$ mm^{-3}) whereas the aged transparent lenses showed only 1·3 MLBs mm^{-2} (calculated density of $5{\cdot}6\times10^2$ mm^{-3}). The Mann–Whitney statistical test for small n supports the trend that the cataracts have more MLBs than the aged transparent lenses ($p=0{\cdot}0003$).

the cataracts have more MLBs than the aged transparent donors lenses ($p=0{\cdot}0003$) (Tables 1 and 2).

To project the number of MLBs per unit volume, the Floderus Eq. (1) was used (Bozzola and Russell, 1999). In 1 mm^3 of tissue, the cataract is predicted to contain $4{\cdot}1\times10^3$ MLBs whereas the aged transparent would contain only $5{\cdot}6\times10^2$.

The Mie scattering theory for coated spheres was used to calculate the predicted scattering efficiency for MLBs (see Section 2). These complex calculations take into account the density of MLBs ($4{\cdot}1\times10^3$ mm^{-3} in the cataract versus $5{\cdot}6\times10^2$ mm^{-3} in the transparent lens), the average diameter of an MLB (2·7 µm, which is the average measured diameter of $2{\cdot}13\pm0{\cdot}64$ µm, $n=117$, corrected for the probability of sectioning through the diameter; Bozzola and Russell, 1999), the refractive index of the cytoplasm, $n=1{\cdot}40$ (Fagerholm et al., 1981; Pierscionek, 1997; Michael et al., 2003), the thickness of the lipid shell (50 nm, which was estimated from this study as 10 layers of 5 nm each), the wavelength of blue and white light (400 and 550 nm, respectively) and the thickness of the lens region in the study (2·6 mm, which is the thickness of the embryonic, fetal and juvenile nuclei; Taylor et al., 1996). The most important parameters are the refractive indices of the particle. The critical parameter for the calculations is

Table 2
Comparison of theoretical predictions to experimental data

	Volume fraction of aged transparent lenses	Volume fraction of cataractous lenses	Particle size (μm)
Theoretical predictions by van den Berg	3×10^{-6} to 6×10^{-6}	5×10^{-5}	1·38
Gilliland et al., 2001	3×10^{-6}	3×10^{-5}	2·36
Current study	3×10^{-6}	2×10^{-5}	2·13
Average of measurements in above two studies	3×10^{-6}	3×10^{-5}	2·25

Theoretical interpretations of light scattering experiments suggest that particles sized 1·38 μm in diameter might exist, occupying a volume fraction between 3×10^{-6} and 6×10^{-6} of the aged transparent lens and 5×10^{-5} of the cataract. A previous study of the equatorial plane and the current study of a plane containing the optic axis demonstrate that particles of size 2·25 μm diameter do in fact exist, occupying a volume fraction of 3×10^{-6} of the aged transparent lens and 3×10^{-5} of the cataract. The Floderus equation was used to determine the volume fraction of the MLBs. The number of MLBs per unit area, the section thickness and the average diameter of an MLB led to a determination that there are approximately 7·5 times as many MLBs in the cataractous nuclei than in the transparent lens nuclei.

the ratio of the refractive index of the particle interior to the surrounding; thus, values above and below that of the cytoplasm will have similar contributions to the scattering efficiency. For this model calculation to demonstrate the potential scattering of the MLBs, the estimated refractive index of the lipid shell is $n=1{\cdot}50$ (Matsuzaki et al., 2000) and the estimated refractive index of the cytoplasm inside the MLB is $n=1{\cdot}49$ (Michael and Brismar, 2001). This latter value was chosen for this example, because it was derived from measurements of a dense mammalian lens nucleus and is somewhat less than 1·54 reported for fish lens nucleus (Garner et al., 2001). The resultant value for scattering efficiency (Q) is 2·5 for white light (wavelength 550 nm) and 3·3 for blue light (wavelength 400 nm). The scattered light was calculated from Eq. (2). For white light, the calculations indicated that in the cataract MLBs may cause about 15% of light to scatter in the forward direction, whereas in the transparent lens, only 2% of the light is expected to be scattered in the forward direction. For blue light, as much as 20% of light is may be scattered in the forward direction by MLBs in the cataract. The results of this latter calculation are presented as a polar plot (Fig. 7A) and scattering intensity plot (Fig. 7B). The polar plot emphasizes the predicted forward scattering at low angles (mainly less than 10°) from the MLBs and the intensity plot on a log scale emphasizes the rapid drop in intensity as a function of scattering angle.

4. Discussion

The distribution of MLBs in histological sections cut parallel to and including the sagittal plane containing the optic axis appeared to be random for both transparent lenses

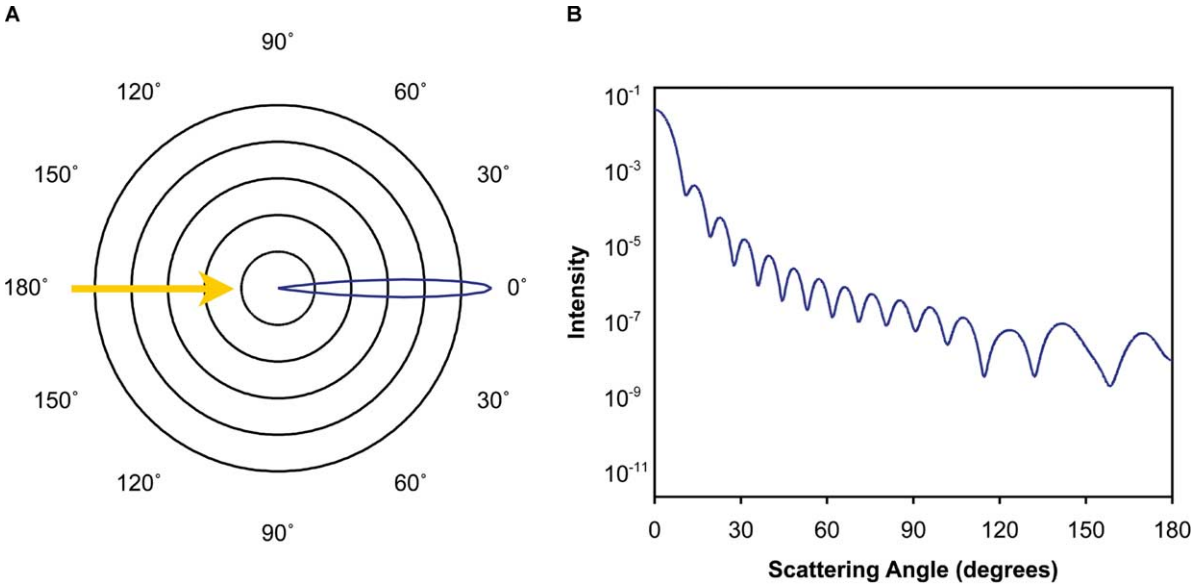

Fig. 7. Calculated Mie light scatter intensity. (A), A polar plot demonstrates that incident light, which travels from left to right (arrow), is scattered by model MLBs with high intensity in the forward direction within a 10° scattering angle. Larger circles represent higher intensity. A vector from the center to any point on the curve represents the intensity and direction of scatter. (B), An intensity plot shows that MLBs cause light to scatter with higher intensity in the forward direction within a 10° scattering angle. In this model calculation MLBs are assumed to be 2·7 μm in diameter with a lipid shell 50 nm thick and 1·50 refractive index. The inside of the MLB is assumed to contain cytoplasm with a refractive index of 1·49, while the surrounding cellular cytoplasm has an assumed refractive index of 1·40.

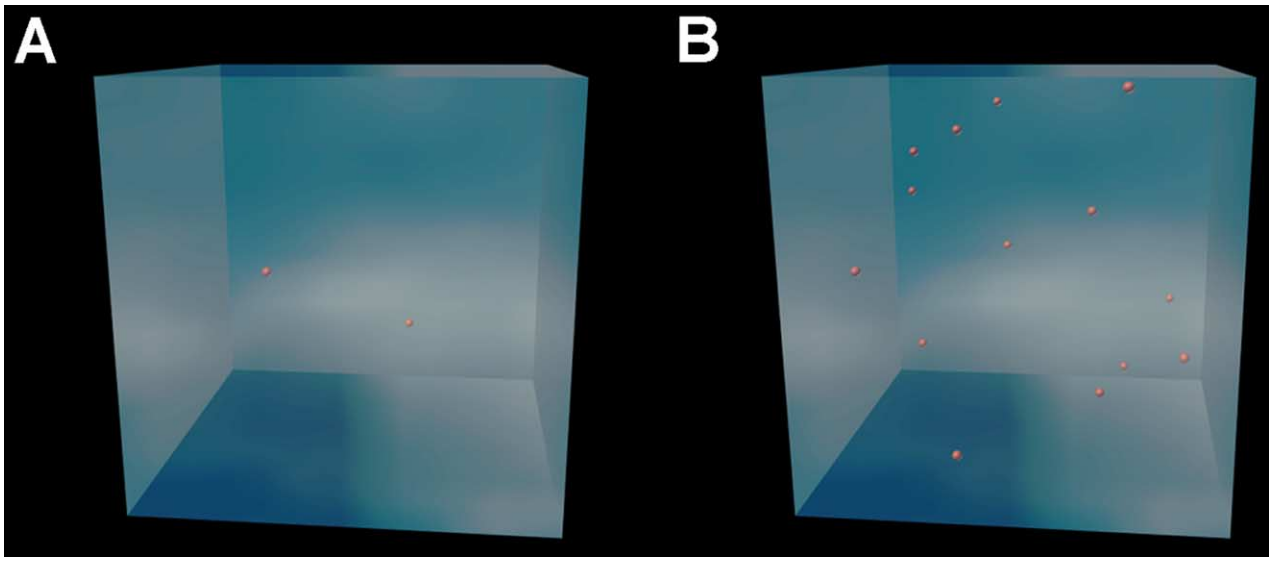

Fig. 8. A diagrammatic representation of MLBs in the aged transparent lens nucleus versus the cataractous nucleus. (A), A model cube with dimensions of 160 μm×160 μm×160 μm is used to demonstrate the approximate volume of tissue in the embryonic nucleus ($4{\cdot}0\times10^{6}$ μm^{3}). Approximately 2 MLBs are found in this volume of tissue in the aged transparent human lens. (B), A similar cube is shown, displaying approximately 14 MLBs in the same volume of tissue in the human age-related cataract. Imagine histological sections through the cubes and the distributions of rare MLBs in the sections.

and cataractous nuclei. The particles were not clustered or enriched within any developmental region. The observed density of MLBs was low, representing a volume fraction of only 3×10^{-6} for the transparent lens nuclei and 2×10^{-5} for the cataractous nuclei (Table 2). When expressed per unit area of histological section examined, the MLBs in the cataracts, at $9{\cdot}6$ MLBs mm^{-2}, were about $7{\cdot}5$ times more numerous than in the transparent lenses, at $1{\cdot}3$ MLBs mm^{-2}. The apparently random distribution and low particle density found in this study was indistinguishable from the study of MLBs in transparent and cataractous nuclei in the equatorial plane (Gilliland et al., 2001). The observed similar distribution and density in the two studies of MLBs in perpendicular planes give support to the hypothesis that the rare MLBs are most likely randomly distributed throughout the entire inner nuclear regions in aged human lenses. The consistently higher density of the MLBs in the cataractous nuclei suggests that they should be considered as sources of excess light scattering.

Although MLBs are extremely rare in both aged transparent lenses and cataractous nulcei, they are in fact much more numerous in cataracts. Just counting the particles gave a 10 times greater frequency in the cataracts as viewed in the equatorial plane (Gilliland et al., 2001) and when normalized per unit area both the current study and previous data agree, indicating that the MLBs are approximately $7{\cdot}5$ times more numerous in the cataracts. This raises the question of how such distinctive spherical objects could have been overlooked in previous morphological studies. To illustrate the difficulty of documenting the MLBs, two cubes are drawn (Fig. 8) with dimensions of 160 μm on a side and are used to represent the approximate volume of tissue in the embryonic nucleus, $4{\cdot}0\times10^{6}$ μm^{-3} (Taylor et al., 1996; Al-Ghoul et al., 2001). In one cube are placed 2 MLBs to represent the density in transparent lenses (Fig. 8A) and in the other cube, 14 MLBS represent the density in cataracts (Fig. 8B). The higher density of MLBs in the cube modeling the cataract is obvious when the whole cube is visualized. However, when sampling the cubes histologically, it is essential to imagine how rarely a particle will be visible in planes only 1 μm thick passing through the cubes. The sampling problem is an order of magnitude more difficult using thin-section TEM. Therefore, these objects have been overlooked mainly because few laboratories have preserved and examined large enough volumes of the inner nucleus to determine particle presence, densities and representative ultrastructural features. The rarity of the MLBs is further emphasized in histological montages (Fig. 2) where no MLBs were observed for either the transparent or cataract samples, even though an area of about $2{\cdot}5\times10^{5}$ μm^{-2} is visible and over 10^{3} cells can be examined. The single MLB in the cataract was not apparent until the montage was greatly extended (Fig. 2D, inset).

The very low density of MLBs raises another question. Is it possible for objects of such low absolute number to produce light scattering sufficient to affect vision? The answer first involves a summary of the structural details of the MLBs. The perfect circular profiles of many of the particles in microtome sections suggest that they are spherical, a conclusion supported by the confocal optical sections through a complex MLB (Fig. 6D). Even when the MLBs contain more than one internal structure, usually one is nearly perfectly spherical (see Fig. 5E, F and G). Although not all MLBs are spherical (see Fig. 5A and B),

they can effectively be approximated as spheres. A distinctive feature of the MLBs in histological sections is the clear band or coat around the sphere. When a lipophilic dye is used, the band is consistently brighter than the adjacent membranes (Fig. 6, Gilliland et al., 2001) indicating that the band is rich in lipids. Recent freeze fracture studies support this proposal: a pellet enriched in MLBs when fractured produced smooth fracture faces devoid of intramembrane protein particles (data not shown; Costello et al., 2003). The ultrastructure of the band in high-resolution TEM images also supports this interpretation (Fig. 4, Gilliland et al., 2001). Typically 3 to 10 layers are seen within the band and each layer has the staining pattern of a lipid bilayer and a thickness of about 5 nm. These thin layers are not thick enough to be formed from the plasma membrane specializations of fiber cells, such as gap junctions, thin symmetric junctions or undulating membranes of the lens (Zampighi et al., 1982; Costello et al., 1989; Zampighi et al., 1989; Costello et al., 1993). Gap junctions of the lens are too thick to be the origin of MLB layers, as each of the two gap junction membranes of the lens is 8 nm in thickness. Likewise, MLB membranes are not likely to be derived from 'thin symmetric junctions,' which contain two closely-associated membranes each 7 nm thick. Because gap junctions are composed of connexins and thin symmetric junctions are probably composed of MIP/Aquaporin0, these integral membrane channel proteins are not expected to be components of the MLB membranes, which are too thin to accommodate the major membrane proteins of the lens. Even the single curved membranes of the undulating surfaces of fiber cells that contain square arrays of MIP/Aquaporin0 are significantly thicker (7 nm) than the MLB layers (5 nm). Therefore, if MLBs do not form from membranes with integral proteins, then they are instead likely to be generated from lipid rich membranes. Somehow lipid components of the membrane are redistributed into a multilayered shell that isolates the MLB interior from the surrounding cytoplasm.

The interiors of the MLBs appear to be similar to the surrounding cytoplasm and are thus probably composed mainly of crystallins (Fig. 4, Gilliland et al., 2001). Because proteins are generally stained non-specifically, the optical density of stain can approximate the density of the protein. MLBs have been observed to have interiors that are both smoother or more textured than the surrounding cytoplasm as well as more densely stained or lighter than the surrounding cytoplasm (Gilliland et al., 2001). Variations in staining density and structure in TEM and LM reported here and previously (Gilliland et al., 2001) support the conclusion that, for many MLBs, the interior staining pattern, and thus the protein density, is different than the surrounding cytoplasm. These internal variations are related to differences in local refractive index and therefore are expected to contribute to light scattering.

To determine the potential contribution of MLBs to light scattering, calculation of the scattering according to Mie (1908) has been presented. This analysis is appropriate for spherical particles that are separated by distances much larger than the wavelength of incident light and that are identical in composition and size. Scattering efficiency per particle is calculated and is dependent on the refractive index ratio of the particle interior to its surroundings and on the ratio of the particle diameter to the wavelength of light. These conditions and parameters can be met approximately. For example, although not all the particles are spherical, most are and the 20% that are more complex can be considered nearly spherical (Fig. 5). The particle sizes also vary over a range of about 1–4 μm but have a fairly narrow distribution around the average diameter of 2·13 μm. The apparent diameter must be corrected by $4/\pi$ to account for the probability that the section will pass through the true diameter. The refractive index of the interior, lipid shell and cytoplasm can be approximated from literature values. The results of the calculations, although only an estimate of the true scattering for idealized identical particles, are revealing. They show that scattering at 400 nm incident wavelength is greater than at 550 nm, that a refractive index difference of particle interior ($n=1{\cdot}49$) to surroundings ($n=1{\cdot}40$) of only 0·09 is sufficient to produce important scattering, and that coated spheres with 2–3 micron diameter have high scattering efficiency. Based on the estimated density of MLBs (Eq. (1)), the intensity of scattering can be calculated (Eq. (2)). For 400 and 550 nm light, the scattering of incident light was 20% and 15%, respectively, for the cataract, and 3% and 2% for the transparent lenses, respectively. The scattering is strongly in the forward direction (Fig. 7) and is likely to affect high acuity image formation at the macula (Thomson, 2001). These results are consistent with the predictions of van den Berg (1997) who suggested that a small volume fraction of micron sized particles could account for the forward scattering of in vitro human lenses.

While it is not known exactly how MLBs form, it is possible that they result from faulty fiber cell elongation that may introduce excess membrane. The excess membrane may be sequestered at the cell interface and over time change composition as proteins migrate from the membrane. This would require a close association with the plasma membrane as is sometimes observed (Fig. 4). Alternatively, MLBs may result during aging from excess cell membranes created after cytoplasmic dehydration and cellular compaction (Al-Ghoul et al., 2001). Closely associated membrane processes may fuse and enclose spherical segments of cytoplasm. Another possibility is that oxidative damage to membranes creates cytoplasmic cell fragments (Babizhayev et al., 1988) which are sequestered by excess membrane that pinches off and coils up to form an MLB. Although the mechanism of these transformations must be quite complex, at least one rat animal model with high oxidative damage has displayed objects similar to MLBs (Costello et al., 2000; Marsili et al., 2004). Moreover, a diabetic rabbit model exhibited some

intriguing multilamellar structures near the cortex/nucleus interface that may be templates or precursors for MLB formation as the cells age (Costello et al., 1993).

Closely packed multiple thin bilayer membranes, 4–5 nm thick as observed in MLBs, are present in a variety of normal and pathological tissues. For comparison, membranes of non-lens MLB-like structures in type II alveolar cells of canine lung have a thickness between 4·3 and 5·4 nm (Ochs et al., 2001). Non-lens MLB-like structures in rat adipose tissue exhibit a regular periodicity of 4 nm (Blanchette-Mackie and Scow, 1981; Blanchette-Mackie and Scow, 1983). In lenses of humans with Type II diabetes, the cortex/nucleus interface contains many globular bodies some having closely packed 5 nm thick membranes (Al-Ghoul and Costello, 1993).

Globular structures sometimes containing multiple membranes have also been observed in the lens cortex. For example, in posterior subcapsular cataracts associated with Type II diabetes, intracellular and extracellular globular bodies have been shown to be the primary cause of opacity (Creighton et al., 1978). Smaller globular bodies (1–4 μm in diameter) in the lens could strongly scatter light, while larger ones (5–20 μm) could scatter and reflect light; together they could account for cortical opacification (Dilley et al., 1976; Costello et al., 1993; de Gottrau et al., 1993). In posterior subcapsular cataracts associated with steroids, Greiner and Chylack have observed multilayed membrane-bound bodies that are 3–4 μm in diameter (Greiner and Chylack, 1979). MLB-like globular bodies have also been observed in the equatorial cortex (Vrensen et al., 1990). While these structures share some structural features with the MLBs described here, the lens nuclear MLBs are unique in their geometry, distribution and location.

Lens and non-lens MLB-like structures may serve a multitude of diverse functions. Non-lens MLB-like globules typically serve as lipid storage locations or secretory organelles. Under normal conditions, they provide lipids for lubrication, such as in joints and on mesodermal cell layers of sliding surfaces (e.g. peritoneum, pericardium and pleural mesothelium). Other non-lens MLB-like structures secrete lipids for the purpose of creating hydrophobic water-protective lipid films, as in mucosa cells of the stomach and epithelial cells of the skin (Hayward, 1979; Schmitz and Muller, 1991). MLB-like structures in the lung store surfactant and ultimately secrete it onto the alveolar surface to lower surface tension (Smith et al., 1972; Coulombe et al., 1988). MLB-like globules are also found as a pathological condition in various tissues. They have been noted to be present in atherosclerosis, Niemann-Pick disease, lecithin:cholesterol acyltransferase deficiency, cholestasis and nerve degeneration (Schmitz and Muller, 1991). Lens MLBs in the nucleus may signal a pathological condition that could have been initiated years earlier. Persons with a high incidence of MLBs may be candidates for age-related nuclear cataract formation.

In order for the aging lens to remain transparent, fiber cells must repair oxidative damage, such as membrane ruptures, damaged proteins and vacuoles due to loss of water and protein fragments. Because mature lens fiber cells have no organelles, no ability to generate mitochondrial energy or synthesize proteins and no lysosomal defense system, they must employ unusual means to combat cellular damage. It is hypothesized that MLBs form as a cellular repair mechanism, collecting damaged membrane and possibly sequestering altered proteins (Vrensen et al., 1990). In this sense they are an unusual replacement for secondary lysosomes or autophagosomes that are not completely removed from the cell (Hariri et al., 2000). Ironically, while these MLBs serve as a protective device, they may also contribute to the development of a pathological condition with aging by transforming into the light scattering particles that cause cataract (Vrensen, 1991; Gilliland et al., 2001). Other changes in the membranes or cytoplasm may also contribute to scattering. As the cytoplasm changes with age, the MLB interiors may change differently because they are isolated by their lipid coats. The result, perhaps over decades of change, is the formation of refractive index gradients around the MLBs that result in particles with very high scattering efficiency.

Acknowledgements

We thank Harold Mekeel for his expert microscopy assistance. Presented in part at the 2002 Annual Meeting of the Association for Research in Vision and Ophthalmology, Ft. Lauderdale, Florida. This project was supported in part by NIH-NEI Research Grant EY08148 (UNC) and Core Grant EY05722 (Duke University).

References

Al-Ghoul, K.J., Costello, M.J., 1993. Morphological changes in human nuclear cataracts of late on-set diabetics. Exp. Eye Res. 57, 469–486.

Al-Ghoul, K.J., Costello, M.J., 1996. Fiber cell morphology and cytoplasmic texture in cataractous and normal human lens nuclei. Curr. Eye Res. 15, 533–542.

Al-Ghoul, K.J., Lane, C.W., Taylor, V.L., Fowler, W.C., Costello, M.J., 1996. Distribution and type of morphological damage in human nuclear age-related cataracts. Exp. Eye Res. 62, 237–251.

Al-Ghoul, K.J., Nordgren, R.K., Kuszak, A.J., Freel, C.D., Costello, M.J., Kuszak, J.R., 2001. Structural evidence of human nuclear fiber compaction as a function of ageing and cataractogenesis. Exp. Eye Res. 72, 199–214.

Babizhayev, M.A., Deyev, A.I., Linberg, L.F., 1988. Lipid peroxidation as a possible cause of cataract. Mech. Ageing Dev. 44, 69–89.

Benedek, G.B., 1971. Theory of transparency of the eye. Appl. Opt. 10, 459–473.

Benedek, G.B., 1997. Cataract as a protein condensation disease: the Proctor Lecture. Invest. Ophthalmol. Vis. Sci. 38, 1911–1921.

Benedek, G.B., Pande, J., Thurston, G.M., Clark, J.I., 1999. Theoretical and experimental basis for the inhibition of cataract. Prog. Retin. Eye Res. 18, 391–402.

Bettelheim, F.A., 1985. Physical basis of lens transparency, in: Maisel, E. (Ed.), The Ocular Lens: Structure, Function, and Pathology. Marcel Dekker, New York, USA, pp. 265–300.

Blanchette-Mackie, E.J., Scow, R.O., 1981. Lipolysis and lamellar structures in white adipose tissue of young rats: lipid movement in membranes. J. Ultrastruct. Res. 77, 295–318.

Blanchette-Mackie, E.J., Scow, R.O., 1983. Movement of lipolytic products to mitochondria in brown adipose tissue of young rats: an electron microscope study. J. Lipid Res. 24, 229–244.

Born, M., Wolf, E., 1959. Principles of Optics, Seventh Ed. Cambridge University Press, Cambridge, UK pp. 759–789.

Boyle, D.L., Takemoto, L.J., 1997. Confocal microscopy of human lens membranes in aged normal and nuclear cataracts. Invest. Ophthalmol. Vis. Sci. 38, 2826–2832.

Bozzola, J.J., Russell, L.D., 1999. Electron Microscopy: Principles and Techniques for Biologists, Second Ed. Jones and Bartlett, Sadbury, MA pp. 330–336.

Costello, M.J., Al-Ghoul, K.J., Oliver, T.N., Lane, C.W., Wodnicka, M., Wodnicki, P., 1993. Polymorphism of fiber cell junctions in mammalian lens, in: Bailey, G.W., Rieder, C.L. (Eds.), Proceedings of the 51st Annual Meeting of the Microscopy Society of America. San Francisco Press, San Francisco, CA, pp. 200–201.

Costello, M.J., McIntosh, T.J., Robertson, J.D., 1989. Distribution of gap junctions and square array junctions in the mammalian lens. Invest. Ophthalmol. Vis. Sci. 30, 975–989.

Costello, M.J., Marsili, S., Lane, C.W., Salganik, R.I., Albright, C.D., Peiffer, R.L., 2000. Cataract formation in a strain of rats selected for high oxidative stress. Microsc. Microanal. 6, 590–591.

Costello, M.J., Freel, C.D., Gilliland, K.O., 2003. Identification of multilamellar bodies in the urea insoluble fraction of human age-related nuclear cataracts. Invest. Ophthalmol. Vis. Sci. 44, 3502.

Coulombe, P.A., Kan, F.W., Bendayan, M., 1988. Introduction of a high-resolution cytochemical method for studying the distribution of phospholipids in biological tissues. Eur. J. Cell Biol. 46, 564–576.

Creighton, M.O., Trevithick, J.R., Mousa, G.Y., Percy, D.H., McKinna, A.J., Dyson, C., Maisel, H., Bradley, R., 1978. Globular bodies: a primary cause of the opacity in senile and diabetic posterior cortical subcapsular cataracts?. Can. J. Ophthalmol. 13, 166–181.

Debye, P., Bueche, A.M., 1949. Scattering by an inhomogeneous solid. J. Appl. Phys. 20, 518–525.

de Gottrau, P., Schlotzer-Schrehardt, U., Dorfler, S., Nauman, G.O., 1993. Congenital zonular cataract: clinicopathologic correlation with electron microscopy and review of the literature. Arch. Ophthalmol. 111, 235–239.

Dilley, K.J., Bron, A.J., Habgood, J.O., 1976. Anterior polar and posterior subcapsular cataract in a patient with retinitis pigmentosa: a light-microscopic and ultrastructural study. Exp. Eye Res. 22, 155–167.

Fagerholm, P.P., Philipson, B.T., Lindstrom, B., 1981. Normal human lens-the distribution of protein. Exp. Eye Res. 33, 615–620.

Freel, C.D., Gilliland, K.O., Lane, C.W., Giblin, F.J., Costello, M.J., 2002. Fourier analysis of cytoplasmic texture in nuclear fiber cells from transparent and cataractous human and animal lenses. Exp. Eye Res. 74, 689–702.

Garner, L.F., Smith, G., Yao, S., Augusteyn, R.C., 2001. Gradient refractive index of the crystalline lens of the Black Oreo Dory (Allocyttus Niger): comparison of magnetic resonance imaging (MRI) and laser ray-trace methods. Vision Res. 41, 973–979.

Gilliland, K.O., Freel, C.D., Lane, C.W., Fowler, W.C., Costello, M.J., 2001. Multilamellar bodies as potential scattering particles in human age-related nuclear cataracts. Mol. Vis. 7, 120–130 (http://www.molvis.org/molvis/v7/a18/).

Gilliland, K.O., Freel, C.D., Lane, C.W., Fowler, W.C., Costello, M.J., 2002. Random distribution of multilamellar bodies in human age-related nuclear cataracts. Invest. Ophthalmol. Vis. Sci. 43, 473.

Greiner, J.V., Chylack, L.T., 1979. Posterior subcapsular cataracts: histopathologic study of steroid-associated cataracts. Arch. Ophthalmol. 97, 135–144.

Hanson, R.A., Hasen, A., Smith, D.L., Smith, J.B., 2000. The major in vivo modifications of the human water-insoluble lens crystallins are disulfide bonds, deamidation, methionine oxidation and backbone cleavage. Exp. Eye Res. 71, 195–207.

Hariri, M., Millane, G., Guimond, M.P., Guay, G., Dennis, J.W., Nabi, I.R., 2000. Biogenesis of multilamellar bodies via autophagy. Mol. Biol. Cell. 11, 255–268.

Hayward, A.F., 1979. Membrane-coating granules. Int. Rev. Cytol. 59, 97–127.

Jedziniak, J.A., Kinoshita, J.H., Yates, E.M., Hocker, L.O., Benedek, G.B., 1973. On the presence and mechanism of formation of heavy molecular weight aggregates in human normal and cataractous lenses. Exp. Eye Res. 15, 185–192.

Jedziniak, J.A., Kinoshita, J.H., Yates, E.M., Benedek, G.B., 1975. The concentration and localization of heavy molecular weight aggregates in aging normal and cataractous human lenses. Exp. Eye Res. 20, 367–369.

Jedziniak, J.A., Nicoli, D.F., Baram, H., Benedek, G.B., 1978. Quantitative verification of the existence of high molecular weight protein aggregates in the intact normal human lens by light-scattering spectroscopy. Invest. Ophthalmol. Vis. Sci. 17, 1–7.

Kerker, M., 1969. The Scattering of Light and Other Electromagnetic Radiation. Academic Press, New York, USA.

Marsili, S., Salganik, R.I., Albright, C.D., Freel, C,D., Johnsen, S., Peiffer, R.L., Costello, M.J., 2004. Cataract formation in a strain of rats selected for high oxidative stress. Exp. Eye Res (doi:10.1016/j.exer.2004.06.008).

Matsuzaki, K., Murase, O., Sugishita, K., Yoneyama, S., Akada, K., Ueha, M., Nakamura, A., Kobayashi, S., 2000. Optical characterization of liposomes by right angle light scattering and turbidity measurement. Biochim. Biophys. Acta 1467, 219–226.

Mätzler, C., 2002. MATLAB functions for Mie scattering and absorption, Version 2 In: IAP Research Report, Institut für angewandte physik, Universität Bern 2002 p. 11.

Michael, R., Brismar, H., 2001. Lens growth and protein density in the rat lens after in vivo exposure to ultraviolet radiation. Invest. Ophthalmol. Vis. Sci. 42, 402–408.

Michael, R., van Marle, J., Vrensen, G.F.J.M., van den Berg, T.J.T.P., 2003. Changes in the refractive index of lens fibre membranes during maturation-impact on lens transparency. Exp. Eye Res. 77, 93–99.

Mie, G., 1908. Beitrage zur optik truber medien, speziell kolloidalen metal-losungen. Ann. Physik. 25, 377.

Ochs, M., Fehrenbach, H., Richter, J., 2001. Ultrastructure of canine type II pneumocytes during hypothermic ischemia of the lung: a study by means of conventional and energy filtering transmission electron microscopy and stereology. Anat. Rec. 263, 118–126.

Pierscionek, B.K., 1997. Refractive index contours in the human lens. Exp. Eye Res. 64, 887–893.

Schmitz, G., Muller, G., 1991. Structure and function of lamellar bodies, lipid–protein complexes involved in storage and secretion of cellular lipids. J. Lipid Res. 32, 1539–1570.

Smith, D.S., Smith, U., Ryan, J.W., 1972. Freeze-fractured lamellar body membranes of the rat lung great alveolar cell. Tissue Cell. 4, 457–468.

Spector, A., 1984. The search for a solution to senile cataracts. Proctor lecture. Invest. Ophthalmol. Vis. Sci. 25, 130–146.

Spector, A., 1995. Oxidative stress-induced cataract: mechanism of action. Fed. Am. Soc. Eur. Biochem. J. 9, 1173–1182.

Tang, D., Borchman, D., Schwarz, A.K., Yappert, M.C., Vrensen, V.F., van Marle, J., DuPre, D.B., 2003. Light scattering of human lens vesicles in vitro. Exp. Eye Res. 76, 605–612.

Taylor, V.L., Al-Ghoul, K.A., Lane, C.W., Davis, V.A., Kuszak, J.R., Costello, M.J., 1996. Morphology of the normal human lens. Invest. Ophthalmol. Vis. Sci. 37, 1396–1410.

Taylor, V.L., Costello, M.J., 1999. Fourier analysis of textural variations in human normal and cataractous lens nuclear fiber cell cytoplasm. Exp. Eye Res. 69, 163–174.

Thomson, D., 2001. Methods of assessing cataract and the effect of opacities on vision. Optometry Today/Optics Today 2001 (http://www.optometry.co.uk/articles2001.htm).

Truscott, R.J., 2000. Age-related nuclear cataract: a lens transport problem. Ophthal. Res. 32, 185–194.

van den Berg, T.J., 1997. Light scattering by donor lenses as a function of depth and wavelength. Invest. Ophthalmol. Vis. Sci. 38, 1321–1332.

van den Berg, T.J., Spekreijse, H., 1999. Light scattering model for donor lenses as a function of depth. Vision Res. 39, 1437–1445.

Vrensen, G., Kappelhof, J., Willekens, B., 1990. Morphology of the aging human lens. II. Ultrastructure of clear lenses. Lens Eye Toxic Res. 7, 1–30.

Vrensen, G., 1991. Discrepancy between onset of early lens changes and onset of senile cataract: the case for cellular defense systems in the human eye lens. Dev. Ophthalmol. 21, 129–133.

Zampighi, G., Simon, S.A., Robertson, J.D., McIntosh, T.J., Costello, M.J., 1982. On the structural organization of isolated bovine lens fiber junctions. J. Cell. Biol. 93, 175–189.

Zampighi, G., Hall, J.E., Ehring, G.R., Simon, S.A., 1989. The structural organization and protein composition of lens fiber junctions. J. Cell Biol. 108, 2255–2275.

Zigler, J.S., 1994. Lens proteins, in: Albert, D.M., Jakobiec, F.A. (Eds.), Principles and Practice of Ophthalmology. W.B. Saunders and Co, Philadelphia, PA, USA pp. 97–113.